land

MDPI

Article

Deconstruction of Dryness and Wetness Patterns with Drought Condition Assessment over the Mun River Basin, Thailand

Sisi Li and Huawei Pi *

Key Research Institute of Yellow River Civilization and Sustainable Development & Collaborative Innovation Center on Yellow River Civilization Jointly Built by Henan Province and Ministry of Education, Henan University, Zhengzhou 475001, China
* Correspondence: huawei.pi@wsu.edu

Abstract: Agriculture is one of the dominant industries in the Mun River Basin, but farmlands are frequently affected by floods and droughts due to the water resource management mode of their rainfed crop, especially in the context of climate change. Drought risk assessment plays an important role in the Mun River Basin's agricultural sustainable development. The objective of this study was to identify the tempo-spatial variation in dryness and wetness patterns; the drought intensity, frequency, and duration; and the potential causes behind drought using the methods of the standardized precipitation evapotranspiration index (SPEI), ensemble empirical mode decomposition (EEMD), correlation analysis, and the Pettitt test over the basin. Results showed that the Mun River Basin underwent a drying climate pattern, which is explained by the significant decreasing trend of SPEI_12M during the study period. In addition, the downstream area of the Mun River Basin was subjected to more intense, extreme dryness and wetness events as the decreased amplitude of SPEI_12M and SPEI_3M was higher than that over the upper and middle reaches. Drought intensity presented a remarkable decadal variation over the past 36 years, and an average 7% increase per decade in the drought intensity was detected. Besides, there have been more mild and moderate droughts frequently appearing over the Mun River Basin in recent decades. For the underlying causes behind the drought condition, on the one hand, the shortened precipitation day over the rainy season accounted more for the intense drought events than the precipitation amount. On the other hand, El Nino Southern Oscillation (ENSO)-brought sea surface temperature anomalies aggravated the potential evapotranspiration (ETr), which might be closely related to the drought intensity and frequency variation. These tempo-spatial maps of dryness and wetness and drought occurrence characteristics can be conducive to local stakeholders and agricultural operators to better understand the agriculture industry risks and vulnerabilities and properly cope with pre-disaster planning and preparedness and post-disaster reconstruction over the Mun River Basin.

Keywords: drought intensity; SPEI_12M; potential evapotranspiration; precipitation days; Mun River Basin

Citation: Li, S.; Pi, H. Deconstruction of Dryness and Wetness Patterns with Drought Condition Assessment over the Mun River Basin, Thailand. *Land* **2022**, *11*, 2244. https://doi.org/10.3390/land11122244

Academic Editors: Assefa M. Melesse, Lulseged D. Tamene and Berhan Gessesse Awoke

Received: 12 November 2022
Accepted: 5 December 2022
Published: 9 December 2022

1. Introduction

As an extreme abiotic stress, drought poses a serious threaten to crop yield and the vegetation-growing environment [1–4], as well as having devastating impacts on regional economic, environmental, and human well-being as a result of the characteristics of long duration, wide-range influence, and great destructive power, and is particularly widespread in most regions of the world with global warming [5–9]. In addition, drought is arguably differentiated from other disasters by its complex and diverse impacts, leading to heavy agricultural and economic damages and losses [10–13].

An increasing number of studies have established how drought has changed in response to climate change, covering subjects from drought index construction [14–17], drought monitoring and forecast [18–20], drought-induced disaster impact investigation [21,22], and specific vegetation response to droughts [23,24] to drought occurrence

analysis and risk assessment over particular watersheds [25,26], which are essential for drought emergency project formulation and agricultural irrigation system optimization. In particular, rapid progress has been made in the spatial and temporal pattern of droughts, drought-related phenomena, and mechanism investigation. Jiao et al. (2021) [27] applied multi-sensor remote sensing to explore drought phenomena and mechanisms, including drought trends, flash drought, and post-drought recovery. Naumann et al. (2018) [3] discussed how drought conditions developed under different levels of global warming and highlighted that two-thirds of the population would experience intense drying conditions. Dai et al. (2020) [28] assessed agricultural drought risk and pointed out that there was a significant increase in agricultural drought risk over the Pearl River Basin. King et al. (2020) [29] examined that the primary reason for the long-lasting dry conditions was the negative impacts of the Indian Ocean dipole over Australia. A growing body of studies believes that the earth is already experiencing more intense and frequent drying conditions with an enormous economic loss for people and irretrievable impacts on ecosystems, whereas some papers have suggested that the drying is still "controversial," especially for long-term trends of drought intensity and frequency variation. A wetting tendency was observed during recent decades in some typical regions, such as the source region of the Yellow River and the Yangtze River [1,30,31], Northwest China [1,12], the Huang-Huai-Hai Plain of China [32], the Upper Great Plains and the Ohio River Valley of the United States [33], and Scandinavia and Belarus [34]. Though drought occurred at a great range of scale on the earth, significant regional differences related to drought variation certainly existed. For example, alterations in regional precipitation patterns and evaporative demands because of climate change were complex and heterogeneous that propagated through the land surface to act on soil moisture, streamflow, and vegetation growth and then considerably drove regional dryness and wetness characteristic formation and variation. As a result, it is necessary to identify drought over the watershed scale so as to assess its significant role in safeguarding agricultural production and safety.

The Mun River Basin, occupying an area of about 70,000 square kilometers, is the largest basin in Thailand. Agriculture is one of the dominant industries of the basin. However, agriculture is particularly vulnerable to frequent droughts and floods because of the 90% rain-fed rice cultivation. Previous studies have indicated that precipitation and evaporation associated with drought occurrence have varied substantially in recent decades with global warming over the Mun River Basin. The increasing annual maximum number of consecutive dry days is significantly associated with the decreased annual maximum daily rainfall over the Mun River Basin [35]. Due to the variation in extreme temperature and precipitation, the frequency of droughts will probably show a steady and sustainable increase. Prabnakorn et al. (2019) [36] predicted more serious crop yield losses with the temperature increasing further. As a result, in this study, we presented a detailed assessment of the drought condition, including drought intensity, frequency, and duration, over the Mun River Basin, which are theoretically and practically important in the context of global climate change. In addition, compared to other studies, we were more concerned with precipitation days as the significant variable influencing drought occurrence. Through the understanding of drought, we sought to provide insights to agricultural producers and managers so that they can plan agricultural system, irrigation, and water resource management according to the tempo-spatial characteristics of drought and its inducements.

Drought risk assessment is important for a basin's agricultural sustainable development, as well as the underlying guarantee for the formation of an agricultural drought warning mechanism [37,38]. A better understanding of drought characteristics and improvement of drought-forecasting techniques will not only reduce losses caused by drought and its subsequent impacts but also allow stakeholders enough support to plan appropriate management practices and mitigate the possible risks. Little is known about the drought risk in terms of dryness and wetness patterns within the Mun River Basin, as well as the potential influencing factors behind the drought condition. Many studies have deemed that the intensified drought was due to the rising temperature and high evapotranspira-

tion [39,40]. However, there has been less emphasis on the importance of precipitation on drought event occurrence, particularly in regions with plentiful precipitation, where precipitation is assumed to have little impact on drought. Actually, the impact of precipitation on drought is critical and more complex as a result of the tempo-spatial variation of precipitation in terms of precipitation frequency, intensity, and duration. Consequently, the mechanism of the drought process is not clear, and there is still a vital question of what significantly affects the drought over the Mun River Basin. This needs to be answered and clarified definitely.

The aim of this study is thus to analyze the possible potential causes of meteorological drought and its tempo-spatial characteristics that would contribute to the construction and maintenance of appropriate disaster mitigation systems and agricultural irrigation schemes. We thus estimate different timescale dryness and wetness patterns and drought conditions containing drought intensity, frequency, and duration so as to reveal the possible inducements accounting for a drought change over the Mun River Basin, Thailand. Knowledge concerning effective drought monitoring is critical not only to better understand local extreme events' uncertainty with climate change but also to provide vital information for drought management and mitigation.

2. Study Area

The Mun River Basin located northeast of Thailand spans from 14° N–16° N to 101°30′ E–105°30′ E, with a drainage area of about 71,000 km^2 [41] (Figure 1). The region is surrounded by several mountains and a plateau range in the southwest, and it is a vast plain in the central and eastern parts. Within the subtropical humid monsoon climate, the Mun River Basin has obvious wet and dry seasons. The annual rainfall is between 1300 mm and 1500 mm. In the wet and dry seasons, rainfall is about 90% and 10%, respectively [41]. The rainfall gradually increases from west to east of the Mun River Basin, with the peak flow occurring from September to October. The annual average temperature is no less than 18 °C, and the highest and lowest temperatures appear in April and January, respectively. The main crops in this region are rice, cassava, and sweet potato, but their annual crop yield is usually unstable due to the influence of monsoon.

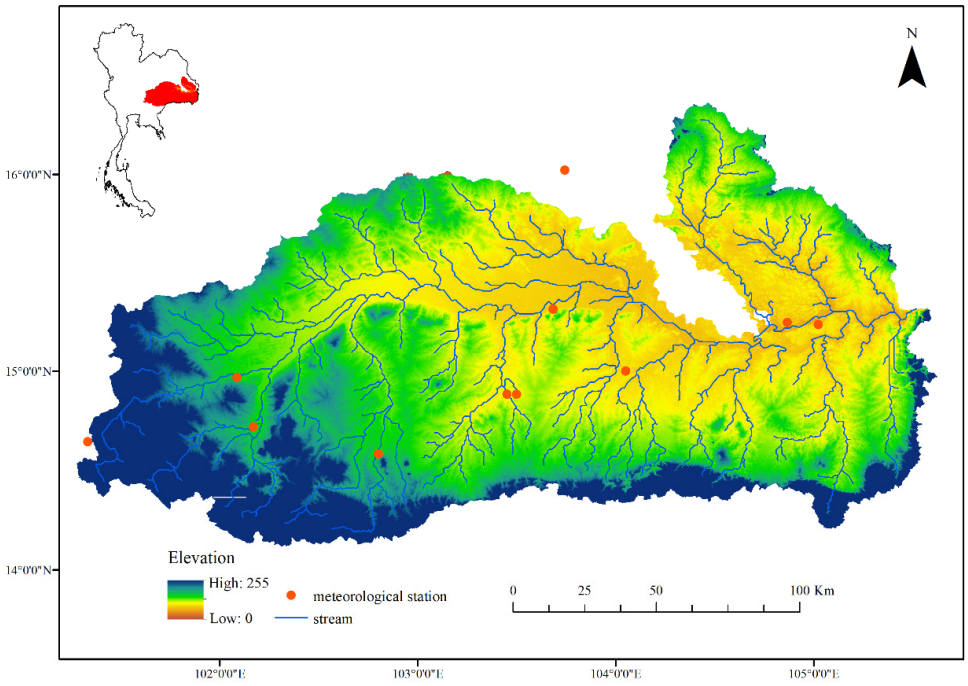

Figure 1. Location of the Mun River Basin based on digital elevation mode (DEM) and the geographic distribution of the 11 meteorological stations.

3. Data and Methods

3.1. Data Processing

Meteorological stations were selected in and around the Mun River Basin from the Thai Meteorology Department (TMD), Thailand (Figure 1). The daily temperature (°C) and precipitation (mm) were used to estimate ETr and the SPEI from 1971 to 2016. First, the quality of the data was assessed and controlled, including extreme removal, data continuity identification, and missed data interpolation [42]. Missing data with a station for not more than 3 days were interpolated using the neighboring stations or days [43]. Ultimately, one of the third station was excluded, and 11 meteorological stations were reserved.

3.2. Methodology

3.2.1. Thornthwaite Equation

The Thornthwaite equation is a widely used method to estimate ETr since it can make a quick estimation using the air temperature and mean daily daylight hours, which can be calculated from the latitude [44,45]. The method uses the following equations to calculate the monthly ETr and also can be a computational check on other more complicated computations of ETr [46,47]:

$$\mathrm{ETr} = 16 * \left(\frac{10 * t}{I}\right)^{\alpha} \tag{1}$$

where t is the mean monthly temperature, I is the annual heat index, and α is an empirical parameter that is determined according to:

$$\alpha = 675 * 10^{-9} * I^3 - 771 * 10^{-7} * I^2 + 1792 * 10^{-5} * I + 0.49239 \tag{2}$$

The annual heat index *(I)* is calculated, as the sum of the monthly heat indices (i):

$$I = \sum_{i=1}^{12} i \tag{3}$$

and

$$i = \left(\frac{t}{5}\right)^{1.514} \tag{4}$$

Potential evapotranspiration is later corrected according to the real length of the month and the theoretical sunshine hours for the latitude of interest, with the formula:

$$\mathrm{ETr\_}corrected = \mathrm{ETr} * \frac{N}{12} * \frac{d}{30} \tag{5}$$

where N is the theoretical sunshine hours for each month and d is the number of days for each month.

3.2.2. Standardized Precipitation Evapotranspiration Index (SPEI)

The standardized precipitation evapotranspiration index is a comprehensive index of water availability and climatic water balance and has significant potential to portray the drought condition with climate change [14]. The characteristics of multiple timescales and convenient calculation processes made it popular in drought risk assessment and dryness and wetness evaluation [31,48].

There are two steps in the calculation of the SPEI. First, the calculation process is based on the difference (D) between monthly precipitation and ETr. D is then accumulated on a predefined time period (e.g., 3 months, 6 months), and the aggregated D is fitted to a probability distribution function. The three-parameter log-logistic distribution was adopted in this study.

The SPEI was calculated at the monthly resolution. The 3-month SPEI (SPEI_3M) and 12-month SPEI (SPEI_12M) were chosen as they could present seasonal and annual scale drought characteristics [49]. Drought intensity, duration, and frequency were investigated based on the value of the 3-month SPEI and 12-month SPEI. The number of months during which the SPEI was <−0.5 was regarded as the drought frequency, and the corresponding mean SPEI absolute value was the intensity. Drought duration was the number of months between drought starting and ending. The longest drought and the total drought duration were also investigated based on SPEI_3M. Table 1 shows the corresponding probabilities of drought occurrence at each level [50,51].

Table 1. Drought grade classification based on the SPEI and corresponding event probabilities.

Drought Grade	SPEI	Probability (%)
Extreme drought	SPEI ≤ -2.0	2.3
Severe drought	$-2.0 <$ SPEI ≤ -1.5	4.4
Moderate drought	$-1.5 <$ SPEI ≤ -1.0	9.2
Mild drought	$-1.0 <$ SPEI ≤ -0.5	17.05
No drought	$-0.5 <$ SPEI ≤ 0.5	17.05

3.2.3. Ensemble Empirical Mode Decomposition (EEMD)

EEMD was determined by considering the deficiency of modal aliasing of the EMD, and it was a noise auxiliary data analysis method [52]. EEMD regards the combination of additional white noise and signals as an entirety, and then, the entirety is divided into modal-consistent IMFs [53,54]. In this study, the EEMD method was used to decompose the SPEI_12M series into various timescale components from 1971 to 2016. The specific steps of EEMD analysis are as follows [55]:

(1) The standard normal distribution white-noise series is added to the targeted data.
(2) The targeted data with additional white noise is decomposed into IMFs.
(3) Repeat steps (1) and (2) n times with a different white-noise series each time.
(4) Obtain the final results based on the ensemble means of corresponding IMFs.

The method of correlation analysis was used to identify the relationship between drought intensity, frequency and ETr, precipitation day, and precipitation amount [56]. The Pettitt test is a nonparametric mutation detection method, and it can detect the mutational point of a hydro-meteorological data series [57,58]. The trends of drought intensity, frequency, ETr, and precipitation were analyzed using this method in this study.

4. Results and Discussion

4.1. Dryness and Wetness Pattern Detection

Figure 2 shows the variation in the mean SPEI_12M (averaged across 11 meteorological stations; Figure 2A) and the intrinsic mode functions (IMFs) of SPEI_12M decomposed by EEMD (Figure 2B–E) from 1971 to 2016 over the Mun River Basin.

SPEI_12M generally displayed a significant decreasing trend from 1971 to 2016 ($p < 0.05$), which illustrates the Mun River Basin experienced a drying climate pattern. In addition, SPEI_12M exhibited a distinct change in phase, even though it decreased significantly. Until the year 1998, SPEI_12M decreased to the lowest value of −1.59, and then, it fluctuated with a slightly increasing trend. During the period of 2008 to 2016, it showed a declining trend again.

There were four IMFs extracted from the average SPEI_12M series over the Mun River Basin. The frequency of the four IMFs went gradually from large to small, which indicated the multi-scales characteristics and different periods of SPEI_12M. The variation in IMF1 showed the highest frequency and apparently represented a 2–3-year periodic. IMF2 was relatively stable and showed a cycle of about 5 years, and the cycle might be associated with the El Nino Southern Oscillation (ENSO). ENSO was strongly related to the abnormal dry conditions in Thailand and frequently resulted in severe crop losses. IMF3 varied with

a cycle of 11.1 years and was much similar to the cycles of sunspots. This indicated that solar activity may indirectly impact the wetness and dryness condition. IMF4 exhibited a temporal trend of dryness and wetness patterns over the Mun River Basin from 1971 to 2016.

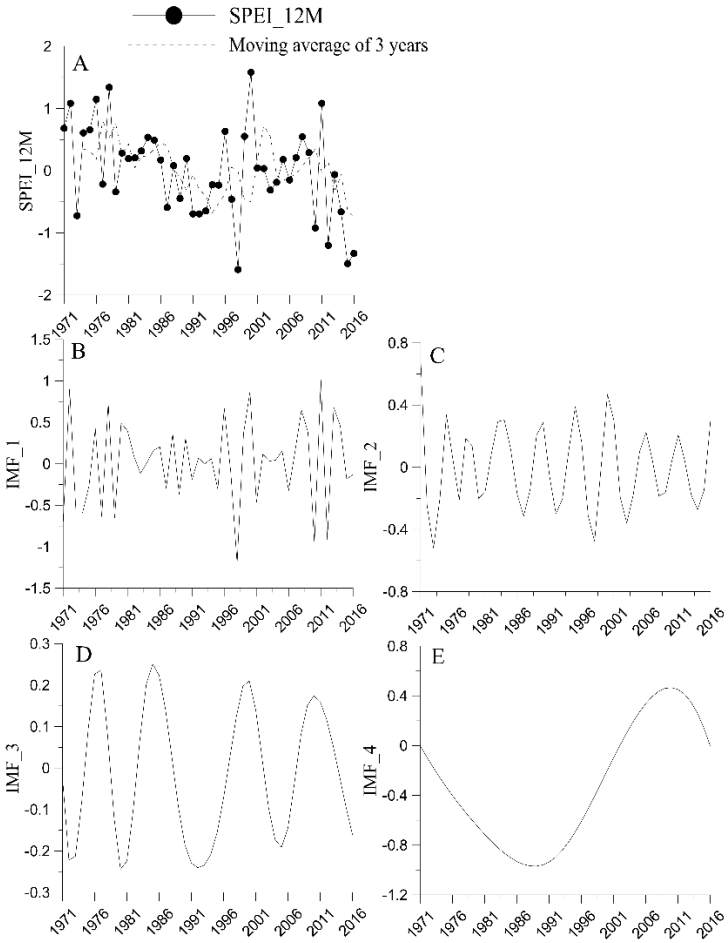

Figure 2. The variation in SPEI_12M (**A**) and the intrinsic mode functions (IMFs) obtained from the SPEI_12M value (**B**–**E**) over the Mun River Basin from 1971 to 2016.

To explore the spatial pattern of dryness and wetness conditions over the Mun River Basin, SPEI_3M and SPEI_12M were investigated at each meteorological station for the period of 1971 to 2016 (Figure 3). Overall, the mean SPEI_3M and SPEI_12M across all stations showed decreasing trends and indicated that the entire Mun River Basin would go through drying conditions. SPEI_3M at approximately 73% of stations and SPEI_12M at 45% stations passed the significance test ($p < 0.05$; Figure 3). This result was similar to the reports by the National Aeronautics and Space Administration (NASA) and Thai officials, and they suggested that severe droughts swept Thailand for nearly 40 years. More similar drying conditions were found in other parts of the world, such as southwestern Europe [34], central Nepal [59], western and southeastern United States [33], the northeast of Australia [60], and the Mongolian Plateau [61]. No doubt that the arid tendency has become a common phenomenon all over the world. The decreasing amplitude of SPEI_12M across stations over the downstream area was higher than that over the upper reaches of the Mun River Basin, which illustrated the downstream area suffered an obvious drying tendency. On the one hand, the downstream area of the Mun River Basin had greater decreasing precipitation compared to the upper reaches. On the other hand, water resource consumption for crop production continuously increased with increasing crop cultivation in recent decades over the downstream area of the Mun River Basin. As a result, evapotranspiration significantly

increased and thus aggravated the dryness condition, which explains the higher decreased slope of SPEI_12M over the downstream area of the Mun River Basin. The decreased amplitude of SPEI_12M was greater than that of SPEI_3M and demonstrated that the wetness and dryness condition variation on a decadal scale was obviously more significant than that on the seasonal scale.

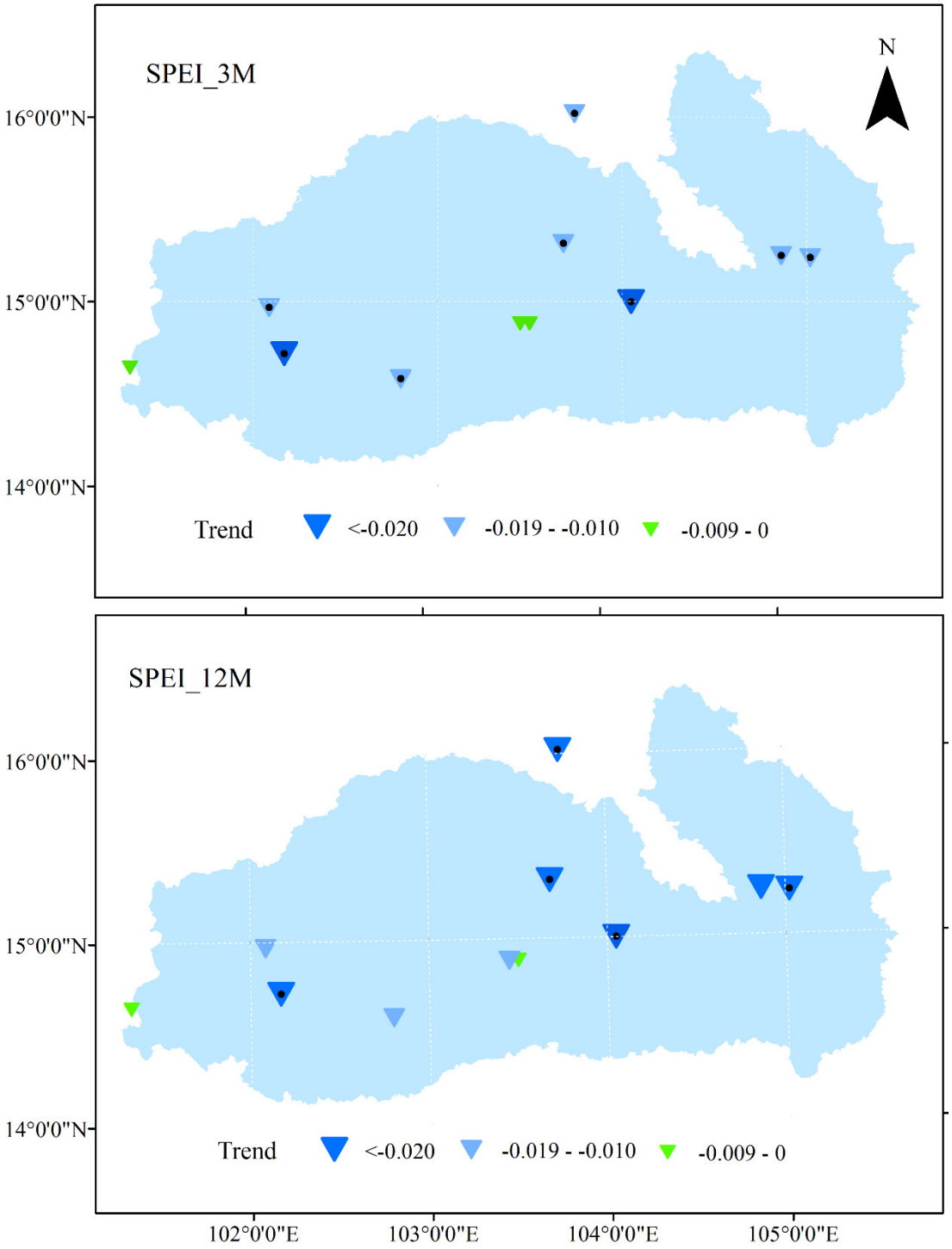

Figure 3. The trends of SPEI_3M and SPEI_12M over the Mun River Basin from 1971 to 2016. The inverted triangles show decreasing trends, and the points show the differences are significant at the 95% confidence interval level based on the Pettitt test.

4.2. Drought Intensity, Frequency, and Duration

In this section, more drought characteristics, such as its intensity, frequency, and duration, were investigated and assessed based on SPEI_12M and SPEI_3M. Figure 4A–E presents the drought intensity of each station from 1971 to 2016 over the Mun River Basin. The study period (46 years) was divided into 5 periods so as to provide more detail and sufficient information about the drought intensity variability.

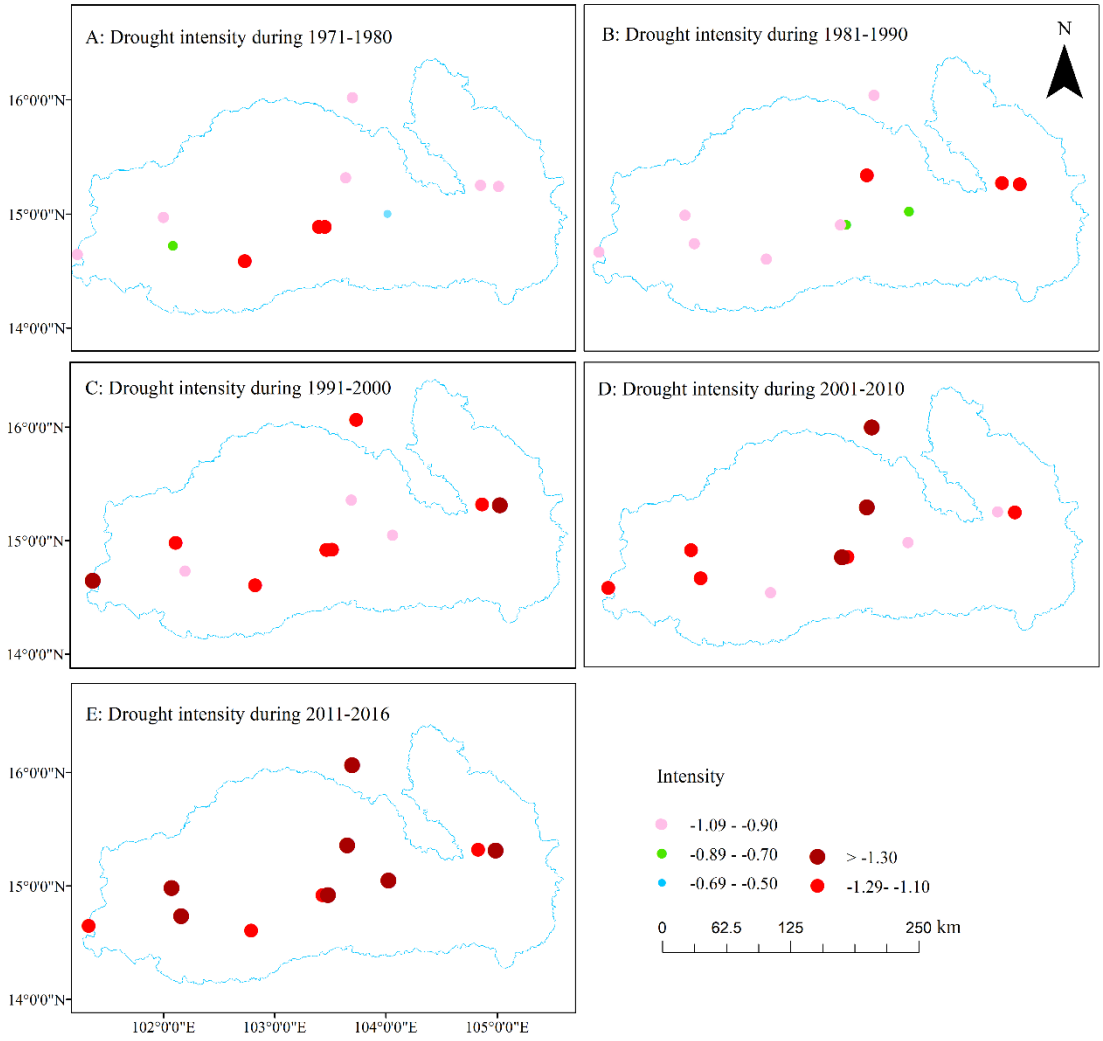

Figure 4. Spatial distribution of drought intensity for every 10 years during the period of 1971–2016 based on SPEI_3M: (**A**)1971–1980, (**B**)1981–1990, (**C**)1991–2000, (**D**) 2001–2010, and (**E**) 2011–2016.

By comparing the spatial distribution of the drought intensity of the 1970s with that of the 1980s, we found that the higher-intensity droughts moved to the downstream area from the middle reaches of the Mun River Basin. In the 1990s, the most higher-intensity drought events occurred over the frontier area, while they shifted from the frontier area to the center area in the 2010s. After 2010, the high-intensity droughts attacked the whole Mun River Basin (Figure 4E). Based on a monthly SPEI of <-0.5 of all stations, we constructed a drought intensity time series from 1971 to 2016 over the Mun River Basin (Figure 5A). The drought intensity series showed an increasing trend and had obvious inter-decadal characteristics. During the period of the 1970s to the 1980s, the drought intensity ranged from 0.66 to 1.14. The drought intensity subsequently increased by 16.4% in the 1990s in comparison to that in the 1980s. The drought intensity reached the highest value of 1.06 after 2010. In addition, the amplitude of the drought intensity fluctuated severely after 1998, indicating that there were more extreme drought events during this period.

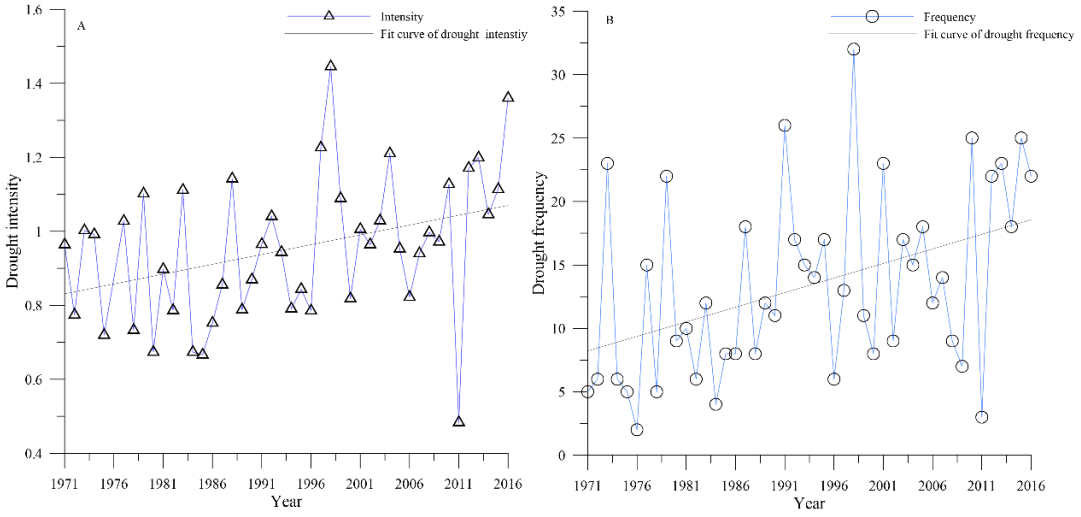

Figure 5. Variation in (**A**) drought intensity and (**B**) frequency over the Mun River Basin from 1971 to 2016.

Mild droughts frequently occurred over the Mun River Basin, with the greatest proportion of mild droughts (over 50%), followed by moderate drought and severe drought from 1971 to 2016 (Figure 6). Though the number of extreme droughts was relatively low and only ranged from 1 to 5 during the study period, their influence was considerable for rice cultivation and output. The drought frequency was higher over the middle-lower area than the upper reaches over the Mun River Basin (Figure 6). Furthermore, a relatively large proportion of moderate drought was detected over the downstream area. For example, the proportion of moderate drought was as high as 60% at the station of Ubon. Similar to the drought intensity being on the increasing trend, the drought frequency also presented a significantly increasing trend ($p < 0.05$; Figure 5B). Reports indicated that fruit production had greatly reduced and that the yield of durian, mangosteen, and longan reduced by almost 50% in 1998 due to prolonged droughts.

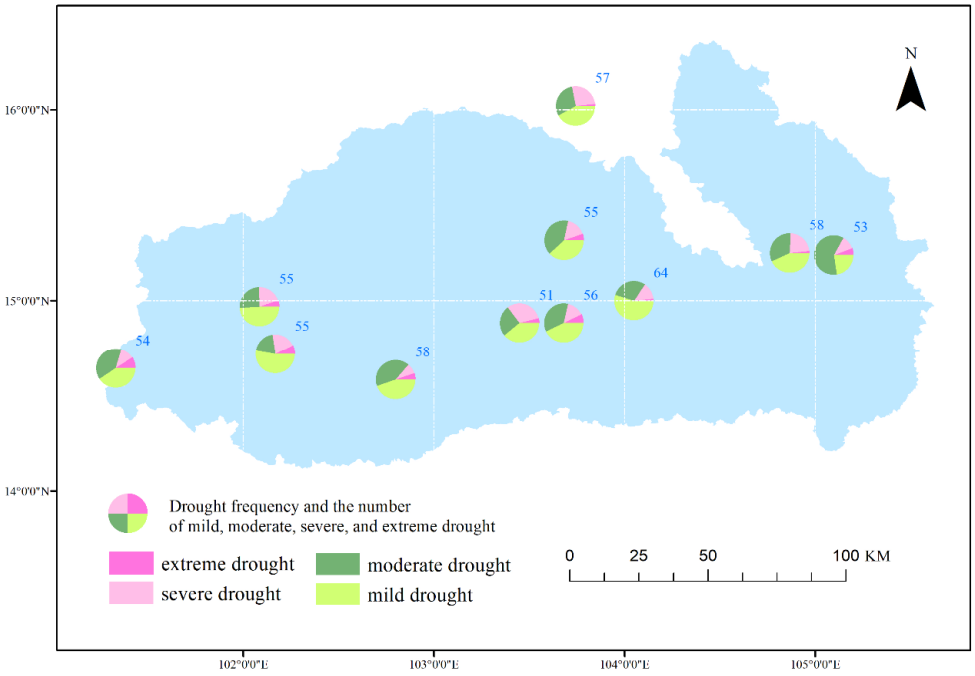

Figure 6. The frequency of mild, moderate, severe, and extreme drought during 1971–2016 over the Mun River Basin, Thailand.

The drought duration also plays an important role in affecting agricultural activities. The longest drought duration (hereafter referred to as the LDD) and the total drought duration (hereafter referred to as the TTD) from 1971 to 2016 over the Mun River Basin are illustrated in Figure 7. We found that the LDD and TDD fluctuated between 11 and 20 and between 137 and 214 months, respectively. A greater LDD of more than 15 months and a TDD of more than 170 months were detected over the upper Mun River Basin, the spatial distribution of the LDD and TDD corresponded to the frequency of extreme drought, and a greater frequency of extreme drought was found over the upper basin. In addition, the LDD occurred after 2010 at about 60% of the stations, and this result echoed the inter-decadal variation in drought intensity.

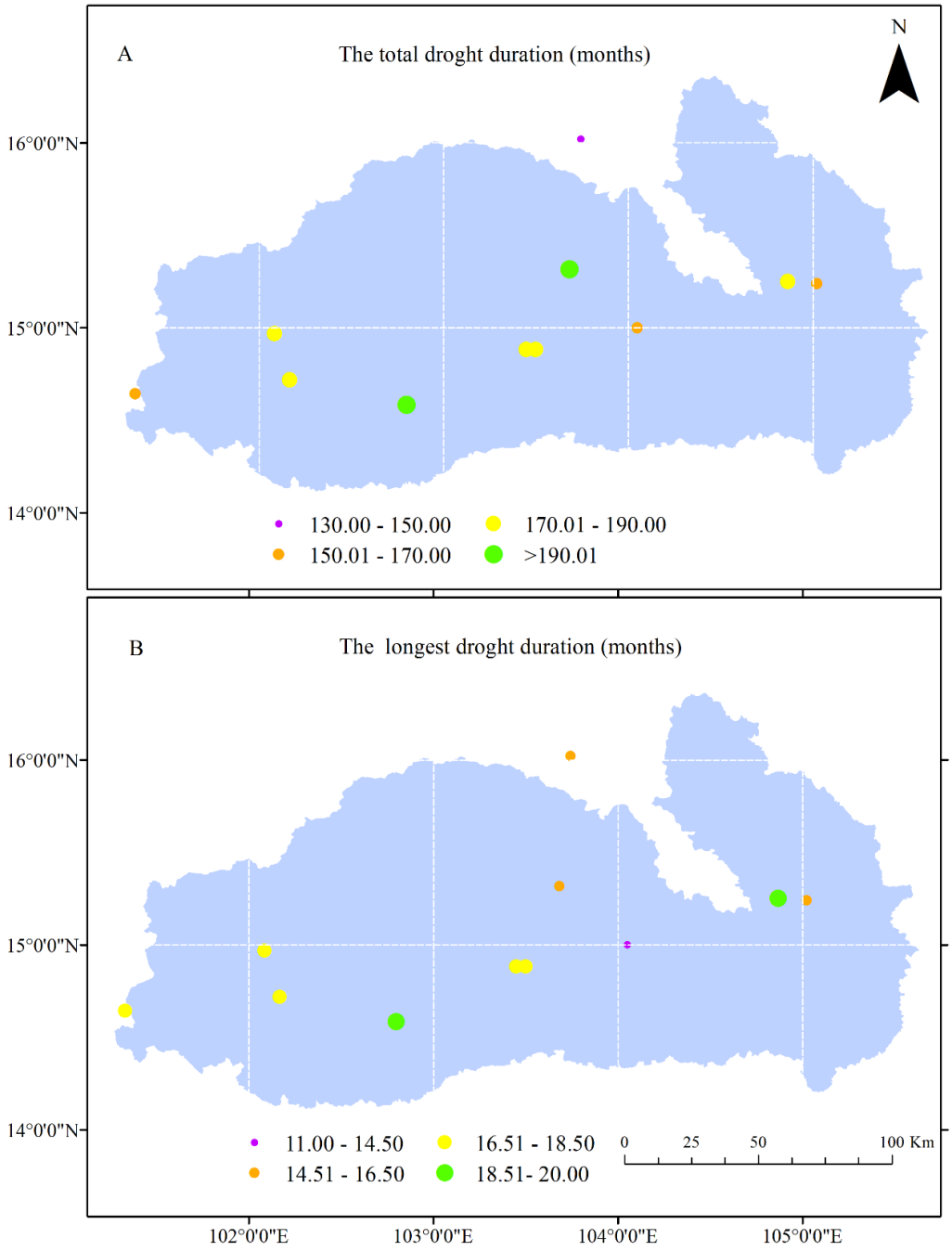

Figure 7. Spatial distribution of (**A**) the total drought duration and (**B**) the longest drought duration during the period of 1971–2016 over the Mun River Basin, Thailand.

4.3. The Potential Influencing Factors for the Drought Condition

In this section, we analyzed the tempo-spatial variation in precipitation and ETr during the study period. Temperature was not factored, because temperature affects drought through its impact on ETr. The seasonal variation in precipitation and ETr was then assessed in a similar way. Finally, the relationship between drought conditions and precipitation and ETr was identified.

The annual variation in precipitation and ETr averaged over the Mun River Basin from 1971 to 2016 is shown in Figure 8. The annual precipitation showed two distinct stages. The annual precipitation decreased by 23.6 mm decade^{-1} until 1993 and then increased after that year (Figure 8A), which was similar to the study of Limsakul and Singhruck (2016) [62]. The average annual precipitation was a little lower (1296.7 mm) from 1971 to 1993 than that in the period of 1993 to 2016 (1359.0 mm). In fact, the highest and lowest values of the annual precipitation may exert an important influence on the precipitation series trend, and they even may reverse the whole trend. For example, the highest precipitation reached 1742.2 mm in 2000. The precipitation increased by 12.3 mm decade^{-1} from 1971 to 2000 but decreased during the period of 2000 to 2016.

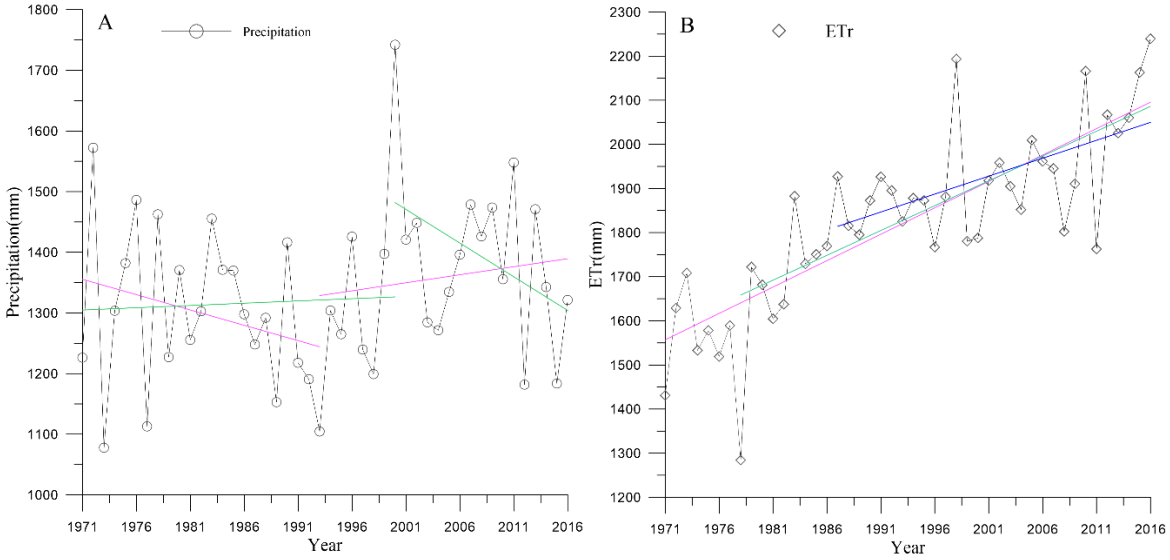

Figure 8. Temporal variation in precipitation (**A**) and ETr (**B**) during the period of 1971–2016 over the Mun River Basin, Thailand. The colorful lines present trends of precipitation and ETr during different time periods.

The annual ETr over the Mun River Basin was significantly upward at a rate of about 112.6 mm decade^{-1} from 1971 to 2016 ($p < 0.05$; Figure 8B). The lowest (1283.8 mm) and highest (2193.6 mm) ETr values were presented in 1978 and 1998, respectively. ETr across the other three time periods all increased based on the linear regression using the Pettitt test (Table 2). The annual ETr was 5% higher over 1987–2016 (1932.0 mm) and 1998–2016 (1974.0 mm) than the period of 1971 to 2016 on average (1826.2 mm; Table 2). We found the ETr series over the Mun River Basin was sensitive to the start dates and the length of records because the line trends of ETr consistently decreased in slope with the starting year change.

Table 2. Mean and trends of ETr across different time periods over the Mun River Basin.

	1971–2016	**1978–2016**	**1987–2016**
Mean (mm)	1826.2	1872.3	1932.0
Trend (mm decade^{-1})	119.7	112.6	81.3
Trend (% decade^{-1})	5.7	7.4	1.6

Figure 9 shifts our attention to the spatial distribution of precipitation and ETr over the Mun River Basin. As the annual variation in precipitation showed with periodic features, we analyzed the spatial variation in precipitation from 1971 to 1993 and from 1994 to 2016 (Figure 9F,G). The precipitation amount decreased at 90% of the stations over the Mun River Basin during the period of 1971 to 1993. On the contrary, the precipitation amount showed increasing trends at 73% of the stations from 1994 to 2016.The more occurrence of ENSO and fewer La Nina events started in the 1970s mostly explain the reduction in precipitation [63,64]. In addition, the significant decreasing rainfall in September was related to a weakening trend of westward-propagating tropical cyclones from the 1970s to the late 1990s [65]. The precipitation days decreased at 80% of the stations (Figure 9D). The precipitation days gradually increased from the upper reaches to the downstream area in the rainy season over the Mun River Basin (Figure 9C). Over the downstream area, the precipitation days were more than 90. Similar to the spatial variation in precipitation days, the precipitation amounts also showed increasing variation from the upper reaches to the downstream area (Figure 9E), and similar results were found by Zhao et al. [66]. Over the Mun River Basin, it was the summer monsoon circulation that dominated precipitation. Much stronger summer monsoon circulation could transport more moisture from the Indian Ocean and Bay of Bengal and subsequently cause anomalously higher rainfall over the northern-central-eastern region than that over the western upper region [67]. Based on our results and previous evidence, the tempo-spatial variation in precipitation over the Mun River Basin is influenced by the variation in atmospheric circulations and its own climate and location. For ETr, it showed an increasing trend with a range from 1394.00 mm to 2009.04 mm during 1971 to 2016 over the Mun River Basin. The high and low values of ETr were distributed across the whole Mun River Basin. In addition, ETr showed larger increased trends over upper reaches and downstream area than that over middle reaches (Figure 9A,B).

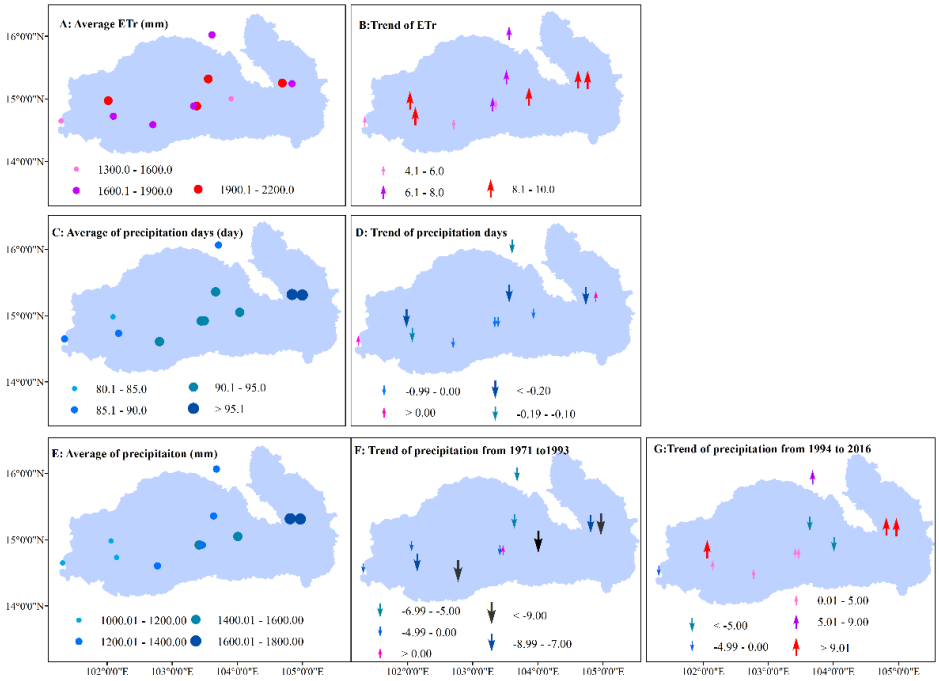

Figure 9. Spatial distribution of ETr, precipitation amount, and precipitation days during the period from 1971 to 2016. The solid circle and arrow indicate the amount and trend, respectively: (**A**) average ETr, (**B**) trend of ETr, (**C**) average precipitation days, (**D**) trend of precipitation days, (**E**) average precipitation amount, (**F**) trend of precipitation from 1971 to 1993, and (**G**) trend of precipitation from 1994 to 2016.

The relationships between ETr, precipitation days, precipitation amount, drought intensity, and drought frequency over the Mun River Basin from 1971 to 2016 were analyzed (Table 3). Both precipitation amount and precipitation days were significantly negatively correlated with drought intensity and drought frequency, respectively, over the Mun River Basin. In particular, the negative correlation coefficient between precipitation days and drought intensity was lower at −0.58, which suggested that the precipitation days contributed more to drought intensity variation over the Mun River Basin (Table 3). On the contrary, ETr exhibited a significant positive correlation with drought intensity and drought frequency, and the correlation coefficients were 0.62 and 0.81, respectively (Table 3). The influence of ETr on drought intensity and drought frequency was much more obvious than that of precipitation days and precipitation amount according to the correlation coefficient absolute value.

Table 3. Correlation between the precipitation amount, precipitation days, ETr, drought intensity, and drought frequency over the Mun River Basin during the period of 1971 to 2016.

	Precipitation Amount	**Precipitation Days**	**ETr**
Intensity	−0.38 **	−0.58 **	0.62 **
Frequency	−0.48 **	−0.42 **	0.81 **

** Significance at a level of 0.01.

The decreasing precipitation days in the rainy season and the increasing ETr significantly influenced the occurrence of drought over the Mun River Basin from 1971 to 2016. The impact of ETr on drought was positive, and the impacts of precipitation on drought were negative, whereas the positive impacts were greater than the negative impacts. As a result, the Mun River Basin went through an intensity drying climate pattern. The precipitation amounts also contributed to drought occurrence, besides precipitation days and ETr. The Mekong River Commission (MRC) once pointed out that monsoon rains in Thailand were not only late frequently for 2 weeks than usual but also retreated early, resulting in shorter precipitation days and less precipitation amount. Even more, the Mun River Basin was dominated by a tropical monsoon climate within obvious dry and wet seasons [40]. Over the dry season, the sunny and dry weather was caused by a large area of downdraft and thus there was reduced convective activity. Both precipitation amount and precipitation days were less over the wet season than over the dry season, which largely explained the higher number of droughts during the dry season. In addition, some studies have demonstrated that ENSO brought high sea surface temperature and thus led to the drying condition worsening over the downstream area of the Mun River Basin [68].

5. Conclusions

The dryness and wetness patterns, drought condition, and the potential reasons behind drought during the period of 1971 to 2016 over the Mun River Basin, Thailand, were assessed and discussed in this study. We found that both SPEI_12M and SPEI_3M at all meteorological stations showed decreasing trends, indicating a drying climate pattern over the Mun River Basin during the study period. Compared to the upstream region, the downstream area suffered more intense, extreme droughts, and this might be connected with the particular location of the downstream area, which is close to the coastal region and more exposed to high sea surface temperature. Drought intensity presented a significant increasing trend with obvious inter-decadal characteristics. Mild drought frequently occurred over the Mun River Basin, and there were striking 32 mild drought events in 1998. The variation in drought frequency and intensity had a significant positive correlation with precipitation days and precipitation amount and were negatively correlated with ETr. According to the correlation coefficients, Etr obviously accounted more for the intense drought condition. The shortened precipitation days contributed more to drought condition variation than the precipitation amount. We deemed that the worsening effects of ETr on the drought condition concealed the retarding effects of precipitation days and precipitation amount

on the drought condition, and that was the main reason that the drought condition was intense over the Mun River Basin.

Due to the complex phenomenon and no universal definition of drought, the mechanism of the drought process is still not clear. With global warming and intense human activities, the spatial differences in the soil moisture content and the variation in streamflow volume should be considered alongside by managers to identify various factors for preventing drought or lessening its effects. This study provided a detailed and complete insights into dryness and wetness patterns and drought monitoring over the Mun River Basin, which is beneficial for drought detection and prevention and in turn conducive to public health and economic development.

Author Contributions: Conceptualization, S.L. and H.P.; methodology, S.L.; validation, H.P.; formal analysis, H.P.; investigation, S.L.; data curation, S.L.; writing—original draft preparation, S.L.; writing—review and editing, S.L. and H.P.. All authors have read and agreed to the published version of the manuscript.

Funding: This study was supported and funded by the fellowship of the China Postdoctoral Science Foundation (2021M690887), the Natural Science Foundation of Henan Province (222300420133), and the University Key Research Projects Plan of Henan Province (22A170005).

Data Availability Statement: The data that support the findings of this study are available from the corresponding author upon reasonable request.

Conflicts of Interest: The authors declare no conflict of interest.

References

1. Li, X.; Zhou, W.; Chen, Y.D. Assessment of Regional Drought Trend and Risk over China: A Drought Climate Division Perspective. *J. Clim.* **2015**, *28*, 7025–7037. [CrossRef]
2. Liu, W.; Sun, F.; Lim, W.H.; Zhang, J.; Wang, H.; Shiogama, H.; Zhang, Y. Global Drought and Severe Drought-Affected Populations in 1.5 and 2 C Warmer Worlds. *Earth Syst. Dyn.* **2018**, *9*, 267–283. [CrossRef]
3. Naumann, G.; Alfieri, L.; Wyser, K.; Mentaschi, L.; Betts, R.; Carrao, H.; Spinoni, J.; Vogt, J.; Feyen, L. Global Changes in Drought Conditions under Different Levels of Warming. *Geophys. Res. Lett.* **2018**, *45*, 3285–3296. [CrossRef]
4. Faiz, M.A.; Zhang, Y.; Zhang, X.; Ma, N.; Aryal, S.K.; Ha, T.T.V.; Baig, F.; Naz, F. A Composite Drought Index Developed for Detecting Large-Scale Drought Characteristics. *J. Hydrol.* **2022**, *605*, 127308. [CrossRef]
5. Wang, W.; Vinocur, B.; Altman, A. Plant Responses to Drought, Salinity and Extreme Temperatures: Towards Genetic Engineering for Stress Tolerance. *Planta* **2003**, *218*, 1–14. [CrossRef] [PubMed]
6. Sheffield, J.; Wood, E.F.; Roderick, M.L. Little Change in Global Drought over the Past 60 Years. *Nature* **2012**, *491*, 435–438. [CrossRef] [PubMed]
7. Trenberth, K.E.; Dai, A.; Van Der Schrier, G.; Jones, P.D.; Barichivich, J.; Briffa, K.R.; Sheffield, J. Global Warming and Changes in Drought. *Nat. Clim. Change* **2014**, *4*, 17–22. [CrossRef]
8. Su, B.; Huang, J.; Fischer, T.; Wang, Y.; Kundzewicz, Z.W.; Zhai, J.; Sun, H.; Wang, A.; Zeng, X.; Wang, G.; et al. Drought Losses in China Might Double between the 1.5 C and 2.0 C Warming. *Proc. Natl. Acad. Sci. USA* **2018**, *115*, 10600–10605. [CrossRef] [PubMed]
9. Páscoa, P.; Gouveia, C.M.; Russo, A.; Ribeiro, A.F. Summer Hot Extremes and Antecedent Drought Conditions in Australia. *Int. J. Climatol.* **2022**, *42*, 5487–5502. [CrossRef]
10. Svoboda, M.; LeComte, D.; Hayes, M.; Heim, R.; Gleason, K.; Angel, J.; Rippey, B.; Tinker, R.; Palecki, M.; Stooksbury, D.; et al. The Drought Monitor. *Bull. Am. Meteorol. Soc.* **2002**, *83*, 1181–1190. [CrossRef]
11. Spinoni, J.; Naumann, G.; Carrao, H.; Barbosa, P.; Vogt, J. World Drought Frequency, Duration, and Severity for 1951–2010. *Int. J. Climatol.* **2014**, *34*, 2792–2804. [CrossRef]
12. Zhang, L.; Zhou, T. Drought over East Asia: A Review. *J. Clim.* **2015**, *28*, 3375–3399. [CrossRef]
13. Peltonen-Sainio, P.; Juvonen, J.; Korhonen, N.; Parkkila, P.; Sorvali, J.; Gregow, H. Climate Change, Precipitation Shifts and Early Summer Drought: An Irrigation Tipping Point for Finnish Farmers? *Clim. Risk Manag.* **2021**, *33*, 100334. [CrossRef]
14. Vicente-Serrano, S.M.; Beguería, S.; López-Moreno, J.I. A Multiscalar Drought Index Sensitive to Global Warming: The Standardized Precipitation Evapotranspiration Index. *J. Clim.* **2010**, *23*, 1696–1718. [CrossRef]
15. Beguería, S.; Vicente-Serrano, S.M.; Reig, F.; Latorre, B. Standardized Precipitation Evapotranspiration Index (SPEI) Revisited: Parameter Fitting, Evapotranspiration Models, Tools, Datasets and Drought Monitoring. *Int. J. Climatol.* **2014**, *34*, 3001–3023. [CrossRef]
16. Mukherjee, S.; Mishra, A.; Trenberth, K.E. Climate Change and Drought: A Perspective on Drought Indices. *Curr. Clim. Chang. Rep.* **2018**, *4*, 145–163. [CrossRef]

17. Tian, L.; Leasor, Z.T.; Quiring, S.M. Developing a Hybrid Drought Index: Precipitation Evapotranspiration Difference Condition Index. *Clim. Risk Manag.* **2020**, *29*, 100238. [CrossRef]
18. Thilakarathne, M.; Sridhar, V. Characterization of Future Drought Conditions in the Lower Mekong River Basin. *Weather Clim. Extrem.* **2017**, *17*, 47–58. [CrossRef]
19. Zhang, Y.; Hao, Z.; Feng, S.; Zhang, X.; Xu, Y.; Hao, F. Agricultural drought prediction in China based on drought propagation and large-scale drivers. Agricultural Water Management. *Agric. Water Manag.* **2021**, *255*, 107028. [CrossRef]
20. Fang, B.; Kansara, P.; Dandridge, C.; Lakshmi, V. Drought Monitoring Using High Spatial Resolution Soil Moisture Data over Australia in 2015–2019. *J. Hydrol.* **2021**, *594*, 125960. [CrossRef]
21. Morán-Tejeda, E.; Ceglar, A.; Medved-Cvikl, B.; Vicente-Serrano, S.M.; López-Moreno, J.I.; González-Hidalgo, J.C.; Revuelto, J.; Lorenzo-Lacruz, J.; Camarero, J.; Pasho, E. Assessing the Capability of Multi-Scale Drought Datasets to Quantify Drought Severity and to Identify Drought Impacts: An Example in the Ebro Basin. *Int. J. Climatol.* **2013**, *33*, 1884–1897. [CrossRef]
22. Pham, Y.; Reardon-Smith, K.; Mushtaq, S.; Deo, R.C. Feedback Modelling of the Impacts of Drought: A Case Study in Coffee Production Systems in Viet Nam. *Clim. Risk Manag.* **2020**, *30*, 100255. [CrossRef]
23. Gupta, A.; Rico-Medina, A.; Caño-Delgado, A.I. The Physiology of Plant Responses to Drought. *Science* **2020**, *368*, 266–269. [CrossRef] [PubMed]
24. Ilyas, M.; Nisar, M.; Khan, N.; Hazrat, A.; Khan, A.H.; Hayat, K.; Fahad, S.; Khan, A.; Ullah, A. Drought Tolerance Strategies in Plants: A Mechanistic Approach. *J. Plant Growth Regul.* **2021**, *40*, 926–944. [CrossRef]
25. Mitchell, K.E.; Lohmann, D.; Houser, P.R.; Wood, E.F.; Schaake, J.C.; Robock, A.; Cosgrove, B.A.; Sheffield, J.; Duan, Q.; Luo, L.; et al. The Multi-Institution North American Land Data Assimilation System (NLDAS): Utilizing Multiple GCIP Products and Partners in a Continental Distributed Hydrological Modeling System. *J. Geophys. Res. Atmos.* **2004**, *109*, D7. [CrossRef]
26. Nasri, M.; Modarres, R. Hydrologic Drought Change Detection. *Nat. Hazards Rev.* **2019**, *20*, 04018022. [CrossRef]
27. Jiao, W.; Wang, L.; McCabe, M.F. Multi-Sensor Remote Sensing for Drought Characterization: Current Status, Opportunities and a Roadmap for the Future. *Remote Sens. Environ.* **2021**, *256*, 112313. [CrossRef]
28. Dai, M.; Huang, S.; Huang, Q.; Leng, G.; Guo, Y.; Wang, L.; Fang, W.; Li, P.; Zheng, X. Assessing Agricultural Drought Risk and Its Dynamic Evolution Characteristics. *Agric. Water Manag.* **2020**, *231*, 106003. [CrossRef]
29. King, A.D.; Pitman, A.J.; Henley, B.J.; Ukkola, A.M.; Brown, J.R. The Role of Climate Variability in Australian Drought. *Nat. Clim. Change* **2020**, *10*, 177–179. [CrossRef]
30. Wang, Y.; Quan, Q.; Shen, B. Spatio-Temporal Variability of Drought and Effect of Large Scale Climate in the Source Region of Yellow River. *Geomat. Nat. Hazards Risk* **2019**, *10*, 678–698. [CrossRef]
31. Li, S.; Yao, Z.; Wang, R.; Liu, Z. Dryness/Wetness Pattern over the Three-River Headwater Region: Variation Characteristic, Causes, and Drought Risks. *Int. J. Climatol.* **2020**, *40*, 3550–3566. [CrossRef]
32. Wang, Q.; Shi, P.; Lei, T.; Geng, G.; Liu, J.; Mo, X.; Li, X.; Zhou, H.; Wu, J. The Alleviating Trend of Drought in the Huang-Huai-Hai Plain of China Based on the Daily SPEI. *Int. J. Climatol.* **2015**, *35*, 3760–3769. [CrossRef]
33. Ficklin, D.L.; Maxwell, J.T.; Letsinger, S.L.; Gholizadeh, H. A Climatic Deconstruction of Recent Drought Trends in the United States. *Environ. Res. Lett.* **2015**, *10*, 044009. [CrossRef]
34. Spinoni, J.; Naumann, G.; Vogt, J.; Barbosa, P. European Drought Climatologies and Trends Based on a Multi-Indicator Approach. *Glob. Planet. Change* **2015**, *127*, 50–57. [CrossRef]
35. Artlert, K.; Chaleeraktrakoon, C.; Nguyen, V.-T.-V. Modeling and Analysis of Rainfall Processes in the Context of Climate Change for Mekong, Chi, and Mun River Basins (Thailand). *J. Hydro-Environ. Res.* **2013**, *7*, 2–17. [CrossRef]
36. Qaisrani, Z.N.; Nuthammachot, N.; Techato, K. Drought Monitoring Based on Standardized Precipitation Index and Standardized Precipitation Evapotranspiration Index in the Arid Zone of Balochistan Province, Pakistan. *Arab. J. Geosci.* **2021**, *14*, 11. [CrossRef]
37. Kuwayama, Y.; Thompson, A.; Bernknopf, R.; Zaitchik, B.; Vail, P. Estimating the impact of drought on agriculture using the US Drought Monitor. *Am. J. Agric. Econ.* **2019**, *101*, 193–210. [CrossRef]
38. Dar, J.; Dar, A.Q. Spatio-temporal variability of meteorological drought over India with footprints on agricultural production. *Environ. Sci. Pollut. Res.* **2021**, *28*, 55796–55809. [CrossRef]
39. Wang, Y.; Wang, S.; Zhao, W.; Liu, Y. The Increasing Contribution of Potential Evapotranspiration to Severe Droughts in the.Yellow River Basin. *J. Hydrol.* **2022**, *605*, 127310. [CrossRef]
40. Prabnakorn, S.; Maskey, S.; Suryadi, F.; de Fraiture, C. Assessment of Drought Hazard, Exposure, Vulnerability, and Risk for Rice Cultivation in the Mun River Basin in Thailand. *Nat. Hazards* **2019**, *97*, 891–911. [CrossRef]
41. Yadav, S.; Babel, M.S.; Shrestha, S.; Deb, P. Land Use Impact on the Water Quality of Large Tropical River: Mun River Basin, Thailand. *Environ. Monit. Assess.* **2019**, *191*, 614. [CrossRef] [PubMed]
42. Deng, H.; Chen, Y.; Chen, X. Driving factors and changes in components of terrestrial water storage in the endorheic Tibetan Plateau. *J. Hydrol.* **2022**, *612*, 128225. [CrossRef]
43. Deng, H.; Pepin, N.C.; Chen, Y. Changes of snowfall under warming in the Tibetan Plateau. *J. Geophys. Res. Atmos.* **2017**, *122*, 7323–7341. [CrossRef]
44. Thornthwaite, C.W. An Approach toward a Rational Classification of Climate. *Geogr. Rev.* **1948**, *38*, 55–94. [CrossRef]
45. Willmott, C.J.; Rowe, C.M.; Mintz, Y. Climatology of the Terrestrial Seasonal Water Cycle. *J. Climatol.* **1985**, *5*, 589–606. [CrossRef]
46. Pereira, A.R.; Pruitt, W.O. Adaptation of the Thornthwaite Scheme for Estimating Daily Reference Evapotranspiration. *Agric. Water Manag.* **2004**, *66*, 251–257. [CrossRef]

47. Yang, Y.; Luo, Y.; Wu, C.; Zheng, H.; Zhang, L.; Cui, Y.; Sun, N.; Wang, L. Evaluation of Six Equations for Daily Reference Evapotranspiration Estimating Using Public Weather Forecast Message for Different Climate Regions across China. *Agric. Water Manag.* **2019**, *222*, 386–399. [CrossRef]
48. Zhou, S.; Wang, Y.; Li, Z.; Chang, J.; Guo, A.; Zhou, K. Characterizing Spatio-Temporal Patterns of Multi-Scalar Drought Risk in Mainland China. *Ecol. Indic.* **2021**, *131*, 108189. [CrossRef]
49. Li, S.; Yao, Z.; Liu, Z.; Wang, R.; Liu, M.; Adam, J.C. The Spatio-Temporal Characteristics of Drought across Tibet, China: Derived from Meteorological and Agricultural Drought Indexes. *Theor. Appl. Climatol.* **2019**, *137*, 2409–2424. [CrossRef]
50. Lloyd-Hughes, B.; Saunders, M.A. A Drought Climatology for Europe. *Int. J. Climatol. J. R. Meteorol. Soc.* **2002**, *22*, 1571–1592. [CrossRef]
51. Chen, S.; Zhang, L.; Liu, X.; Guo, M.; She, D. The Use of SPEI and TVDI to Assess Temporal-Spatial Variations in Drought Conditions in the Middle and Lower Reaches of the Yangtze River Basin, China. *Adv. Meteorol.* **2018**, *2018*, 9362041. [CrossRef]
52. Huang, N.E.; Shen, Z.; Long, S.R.; Wu, M.C.; Shih, H.H.; Zheng, Q.; Yen, N.-C.; Tung, C.C.; Liu, H.H. The Empirical Mode Decomposition and the Hilbert Spectrum for Nonlinear and Non-Stationary Time Series Analysis. *R. Soc. Lond. Ser. A Math. Phys. Eng. Sci.* **1998**, *454*, 903–995. [CrossRef]
53. Liu, Y.; Feng, J.; Ma, Z. An analysis of historical and future temperature fluctuations over China based on CMIP5 simulations. *Adv. Atmos. Sci.* **2014**, *31*, 457–467. [CrossRef]
54. Qian, C.; Yan, Z.; Wu, Z.; Fu, C.; Tu, K. Trends in temperature extremes in association with weather-intraseasonal fluctuations in eastern.China. *Adv. Atmos. Sci.* **2011**, *28*, 297–309. [CrossRef]
55. Jin, J.; Wang, Q.; Li, L. Long-term oscillation of drought conditions in the western China: An analysis of PDSI on a decadal scale. *J. Arid. Land* **2016**, *8*, 819–831. [CrossRef]
56. Yuan, J.; Xu, Y.; Xiang, J.; Wu, L.; Wang, D. Spatiotemporal Variation of Vegetation Coverage and Its Associated Influence Factor Analysis in the Yangtze River Delta, Eastern China. *Environ. Sci. Pollut. Res.* **2019**, *26*, 32866–32879. [CrossRef]
57. Martinez, M.D.; Serra, C.; Burgueño, A.; Lana, X. Time Trends of Daily Maximum and Minimum Temperatures in Catalonia (Ne Spain) for the Period 1975–2004. *Int. J. Climatol. J. R. Meteorol. Soc.* **2010**, *30*, 267–290. [CrossRef]
58. Zuo, D.; Xu, Z.; Liu, X.; Cheng, L. Spatiotemporal Variation and Abrupt Changes of Potential Evapotranspiration in the Wei River Basin. *IAHS-AISH Publ.* **2011**, *350*, 28–37.
59. Dahal, P.; Shrestha, N.S.; Shrestha, M.L.; Krakauer, N.Y.; Panthi, J.; Pradhanang, S.M.; Jha, A.; Lakhankar, T. Drought Risk Assessment in Central Nepal: Temporal and Spatial Analysis. *Nat. Hazards* **2016**, *80*, 1913–1932. [CrossRef]
60. McGree, S.; Schreider, S.; Kuleshov, Y. Trends and Variability in Droughts in the Pacific Islands and Northeast Australia. *J. Clim.* **2016**, *29*, 8377–8397. [CrossRef]
61. Tong, S.; Lai, Q.; Zhang, J.; Bao, Y.; Lusi, A.; Ma, Q.; Li, X.; Zhang, F. Spatiotemporal Drought Variability on the Mongolian Plateau from 1980–2014 Based on the SPEI-PM, Intensity Analysis and Hurst Exponent. *Sci. Total Environ.* **2018**, *615*, 1557–1565. [CrossRef] [PubMed]
62. Limsakul, A.; Singhruck, P. Long-term trends and variability of total and extreme precipitation in Thailand. *Atmos. Res.* **2016**, *169*, 301–317. [CrossRef]
63. Limjirakan, S.; Limsakul, A. Spatio-temporal changes in total annual rainfall and the annual number of rainy days. In Proceedings of the Conference Handbook, Sydney, Australia, 2–5 October 2007; Volume 29, pp. 1–21.
64. Mantua, N.J.; Hare, S.R.; Zhang, Y.; Wallace, J.M.; Francis, R.C. A Pacific interdecadal climate oscillation with impacts on salmon production. *Bull. Am. Meteorol. Soc.* **1997**, *78*, 1069–1080. [CrossRef]
65. Takahashi, H.G.; Yasunari, T. Decreasing trend in rainfall over Indochina during the late summer monsoon: Impact of tropical cyclones. *J. Meteorol. Soc. Japan. Ser. II* **2008**, *86*, 429–438. [CrossRef]
66. Zhao, Z.; Liu, G.; Liu, Q.; Huang, C.; Li, H.; Wu, C. Distribution characteristics and seasonal variation of soil nutrients in the Mun River Basin, Thailand. *Int. J. Environ. Res. Public Health* **2018**, *15*, 1818. [CrossRef]
67. Tangang, F.; Santisirisomboon, J.; Juneng, L.; Salimun, E.; Chung, J.; Supari, S.; Cruz, F.; Ngai, S.; Ngo-Duc, T.; Singhruck, P.; et al. Projected future changes in mean precipitation over Thailand based on multi-model regional climate simulations of CORDEX Southeast Asia. *Int. J. Climatol.* **2019**, *39*, 5413–5436. [CrossRef]
68. Khadka, D.; Babel, M.S.; Shrestha, S.; Virdis, S.G.; Collins, M. Multivariate and Multi-Temporal Analysis of Meteorological Drought in the Northeast of Thailand. *Weather Clim. Extrem.* **2021**, *34*, 100399. [CrossRef]